# CHAPTER 1

# INTRODUCTION

## 1.1 Introduction

One-dimensional (1D) nanomaterials - nanorods, nanowires, nanofibers, nanobelts and nanotubes - have attracted considerable interest due to their novel physical and chemical properties, and potential wide-range application. These 1D nanomaterials can be used as building blocks to assemble new generations of novel nanoscale devices. An important issue in the study and application of these 1D nanomaterials is how to assemble them into highly integrated and hierarchically organized nanostructures growing along one direction. Many researchers and scientists have been made to assemble 1D nanostructures and to optimize these properties [1-2].

Among the various transition metal oxides, tungsten oxide has received wide attention owing to its unique photochromic and electrochromic properties. It is considered as a promising material for a multiple of potential applications including semiconductors, gas sensors, cathode materials for secondary batteries, solar energy devices, photocatalysts, erasable optical storage devices and field-emission devices. Generally, monoclinic tungsten oxide structure (m-$WO_3$), is used in gas sensors. In particular, the hexagonal tungsten oxide structure (h-$WO_3$) as tunnel structure is of great interesting. Small ions such as $H^+$, $Li^+$, $Na^+$, $K^+$, etc, can be inserted in an

intercalation host of tunnel h-$WO_3$ to produce tungsten oxide bronzes. The energy was obtained by the reversed reaction. Therefore, it is a candidate for electrocatalysis for hydrogen evolution reaction of fuel cells, and cathodes for secondary Li-ion batteries. Meanwhile, with the development of 1D nanostructured materials, dimensionality and size of the materials have also been regarded as critical factors that may bring some novel and unexpected properties. Thus the synthesis of $WO_3$ with well-controlled dimensionality, size and crystal structure is of special interest and great importance [1-7].

Various methods have been developed for the synthesis of 1D $WO_3$ nanostructure, such as hydrothermal/solvothermal synthesis [3, 6, 8-11], hot-wire chemical vapor deposition [12], spray pyrolysis [4], template mediated synthesis [13], sol-gel method [14] and microemulsion technique [15]. Among these, synthesis under hydrothermal conditions is a low-temperature, environmentally benign and low-cost route for preparation of nanosized oxide materials, and is becoming an increasingly attractive method [16].

In the present research, $WO_3$ nanostructure was synthesized using hydrothermal method. A number of reaction conditions such as acidity, time and temperature were used to control the synthesis of $WO_3$ nanostructure with different aspect ratios. The effects of different reaction conditions on the final products will be systematically investigated.

## 1.2 Tungsten oxide

### 1.2.1 Physical Properties [17]

| | |
|---|---|
| IUPAC name | Tungsten trioxide |
| Other names | Tungstic anhydride, Tungsten (VI) oxide, Tungsten oxide |
| Molecular formula | $WO_3$ |
| Molar mass | 231.84 g/mol |
| Appearance | light-green powder |
| Density | 7.16 g/cm$^3$ |
| Melting point | 1473 °C |
| Boiling point | ~1700 °C |
| Solubility in water | insoluble |

### 1.2.2 Structure of Tungsten Oxide [18]

#### 1.2.2.1 General characteristics of $WO_3$ and transition metal oxides [18]

An amorphous ($\alpha$)–$WO_3$ film has a definite ionic and electronic conduction. It has large opened porous and it is constituted by clusters. The clusters are built from no more than 3-8 $WO_6$–octahedra, linked together by corners or edges and in the complete structure of the film connected with one another by W-O-W bonds or water bridges. The voids observed within the film are the result of random packing of the clusters and mostly give the open structure that is normally filled with molecular water taken from the air. The presence of water is necessary to stabilize the

microcrystalline structure of an α–$WO_3$ film with the open pore structure. The ionic conduction of an α–$WO_3$ film is ensured by proton transport through channels or water bridges in pores, but the electronic conduction is done by the clusters linked together by W-O-W bonds [18].

The binary W-O system is rather complex with a large number of phases. The most stable $WO_3$ phase at room temperature has a monoclinic structure, but this phase transforms to an orthorhombic or a tetragonal phase at higher temperatures. Many different structures of tungsten oxide clusters have been investigated. The trioxide, $WO_3$ can crystallize in many polymorphs with various crystal structures [18].

Generally $WO_3$ and related electrochromic materials are divided into three main groups with regard to bulk crystalline structures. (i) Perovskite-like, such as $WO_3$, $MoO_3$, $SrTiO_3$; (ii) Rutile-like, $TiO_2$, $MnO_2$, $VO_2$, $RuO_2$, $IrO_2$ and $RhO_2$ ; (iii) Layer and block structures forming a somewhat undefined group, such as $V_2O_5$, $Nb_2O_5$ [18].



#### 1.2.2.2 Perovskite-like Structure [18]

The tungsten oxides consist of $WO_6$ –octahedra arranged in various sharing (corners, edges, planes) configurations. The main differences between the phases are shifts in the position of the W atoms within the octahedral, and variations in W-O bond lengths. The simplest form with a general composition, $WO_3$ or $LiWO_3$,

is the (defect) perovskite structure shown in Figure 1.1a. The W ions occupy the corners of a primitive unit cell, and O ions bisect the unit cell edges. The central atom is absent at the moment and will be denoted as Li or Na after the intercalated ions occupying symmetric positions. Each W ion is surrounded by six equidistant oxygen ions (Figure 1.1a, part II). The stable monoclinic $WO_3$ can have a $ReO_3$-type structure (corner-sharing arrangement of octahehra). An infinite array of corner- sharing $WO_6$ – octahedra is formed like in Figure 1.1b. These octahedras are in planes perpendicular to the [001] hexagonal axis and they form four membered rings in the xy or (001) plane. These layers are stacked in arrangement and are held together by weak van de Waal´s force. The stacking of such planes along the z axis leads to the formation of tunnels between these octahedras (Figure 1.1c). In the extended tunnel small ions can stay or move in case of an exterior force. This may present the possibility of ionic transport and intercalation in the structure, and a mechanism for electrochromic materials [18].

#### 1.2.2.3 Rutile-like Structure [18]

The ideal rutile-like structure can be thought of as built from almost $MeO_6$ (Me=metal; O=oxygen) –octahedra units forming infinite edge-shared chains which can create vacant tunnels (Figure 1.1d). Several oxygen deficient $WO_{3-X}$ phases (Magneli phases) have been identified as the shear phase containing edge-shared octahedral. In the substoichiometric tungsten oxides, $W_{18}O_{49}$ ($WO_{2.72}$) and $W_{20}O_{58}$ ($WO_{2.90}$), the shortage of oxygen is compensated by the formation of edge-sharing

octahedra. The distances between the nearest W-W are widely distributed in these crystals. From Nanba et al. the W-O nearest neighbor distance is ~0.2 nm. The W-W nearest neighbor distance is in the range 0.37-0.40 nm. The structure radial distribution 0.73 nm and all the above can be reconciled with a hexagonal structure and $WO_6$–octahedra building blocks [18].

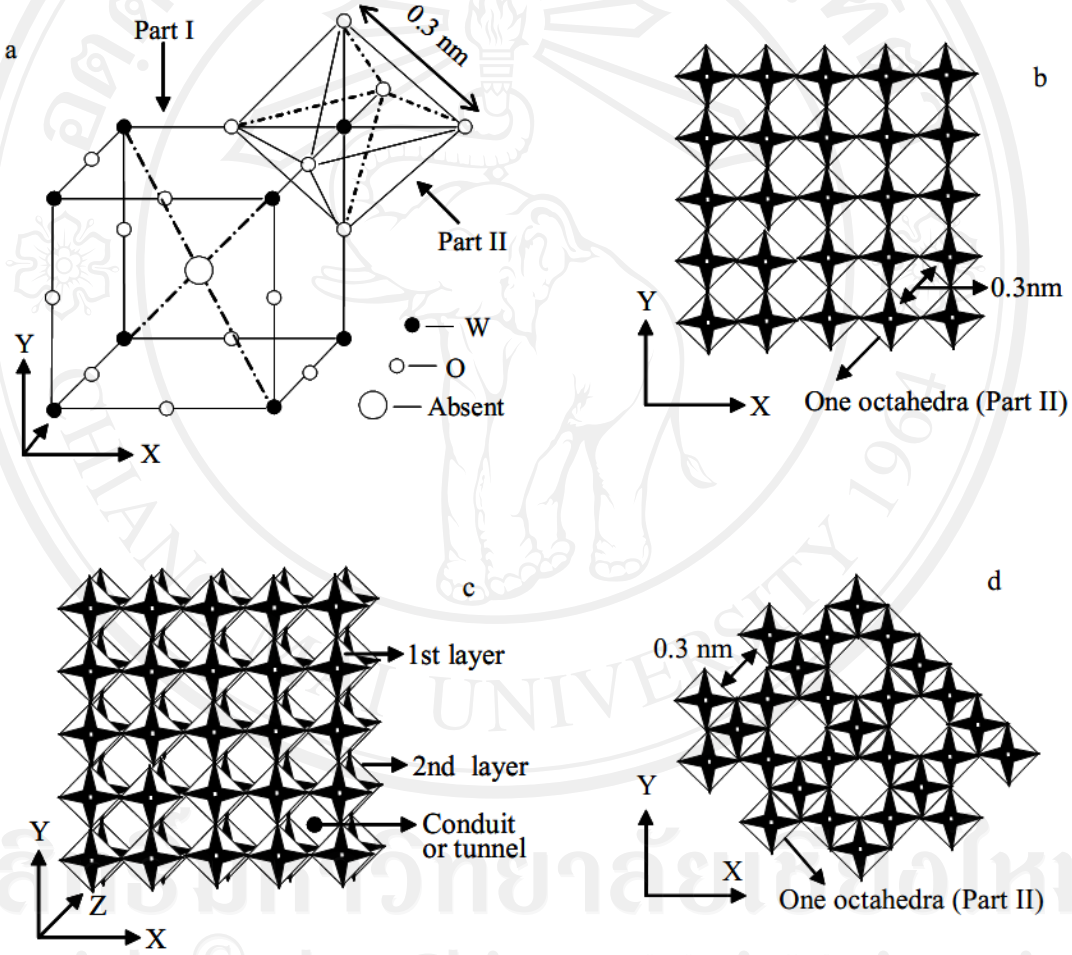


Figure 1.1 (a) Unit cell for the perovskite lattice (Part I) and octahedral symmetries (Part II) in the perovskite structure; (b) One layer of the monoclinic $WO_3$ structure in the corner-sharing arrangement of octahedra ($ReO_3$-type); (c) The monoclinic $WO_3$ structure ($ReO_3$-type); (d) One layer of the monoclinic $WO_3$ structure in the edge-sharing arrangement of octahedra [18].

#### 1.2.2.4 Tungsten oxide hydrates [18]

Tungsten oxide hydrates, $WO_3.nH_2O$, are common compounds, synthesized from sol-gel, even vacuum methods. They can form layers built up by corner sharing ($WO_6$) octahedra, with water molecules between these layers. Its structure is similar to Figure 1.1. The formation of such layered structures from solute aqueous precursors is explained as follows. Hydrous oxides are precipitated upon the acidification of tungstate $(WO_4)^{2-}$, where neutral precursors $(H_2WO_4)^0$ are formed (Figure 1.2a). Coordination expansion leads to the formation of six-fold coordinated $W^{6+}$ via the nucleophilic addition of two water molecules (Figure 1.2a and b). However as the preferred coordination of $W^{6+}$ is known to be mono-oxo (W=O, mono-oxolation), the neutral precursor should be $[WO(OH)_4(OH_2)]^0$. One water molecule is bonded along the z-axis opposite to the W=O bond while the four OH groups are in the equatorial xy plane (Figure 1.2b, c). In order to decrease electrostatic repulsions between highly charged cations, $W^{6+}$ shifts toward the terminal oxygen (W=O bond) leading to strongly distorted $WO_6$ octahedra. Oxolation along equivalent x and y directions leads to the formation of the layered amorphous $WO_3.nH_2O$ gels or crystalline $WO_3.2H_2O$ and $WO_3.H_2O$ phases. The $WO_3.2H_2O$ and $WO_3.H_2O$ can be obtained via the acidification of a tungstate solution $Na_2WO_4$ through a proton exchange resin. $WO_3.H_2O$ can be obtain with a 100 $^oC$ heated environment during synthesis, and its structure is like in Figure 1.1c [18].



In the case of hydrothermal synthesis, the dielectric constant of water decreases as the temperature increases. Electrostatic repulsions between highly charged $W^{6+}$ ions become stronger leading to the formation of more open structures

such as hexagonal $WO_3.1/3H_2O$ (Figure 1.3a). In the structures of hexagonal $WO_3.1/3H_2O$ there is a corner which was occupied by a water molecule. These octahedra shared by four oxygens and form hexagonal assemblies in the xy plane. The layers stack along the z axis and are alternatively shifted by a/2 (Figure 1.3b). Figure 1.3a shows a structural model based on hexagonal $WO_3$, in which three- and six-membered rings of octahedra are displayed in the projected X-Y plane and four-membered rings are parallel to the vertical Z direction [18].

The three-member rings (Figure 1.3) can be ascribed to the $W_3O_9$ molecules produced during evaporation and sputtering, and such molecules can be tied together to form six-member rings. Amorphous peroxotungstic acids have this kind of structure which is made of hydrogen bonded polyanionic species close to the paratungstate polyanion $[W_{12}O_{42}H_2]^{10-}$ and so do the $WO_3.1/3H_2O$ [18].

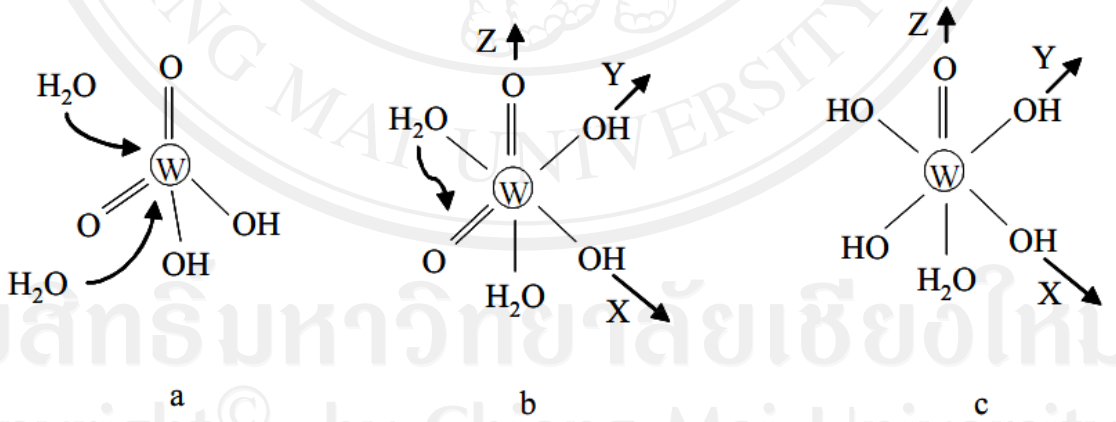


Figure 1.2 Formation of $WO_3.nH_2O$ from the neutral precursor $[H_2WO_4]^0$ [18]

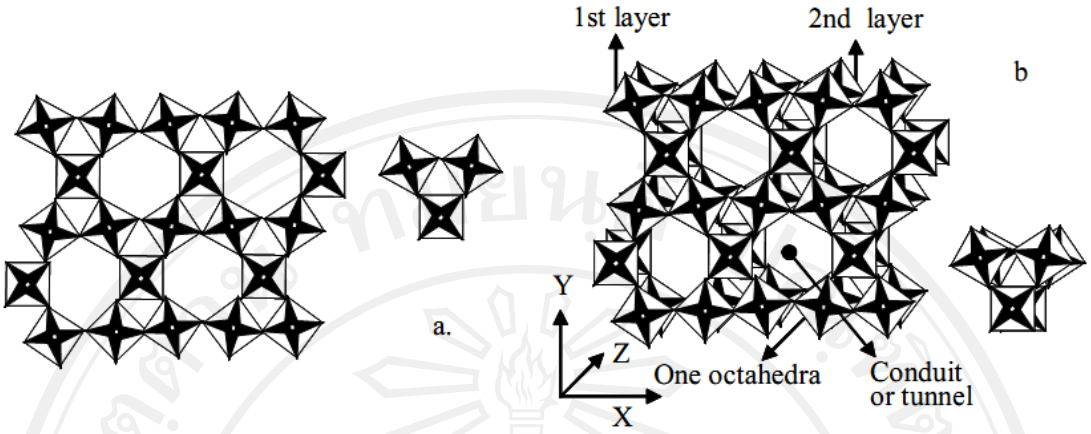


Figure 1.3 (a) The six membered rings of ($WO_6$) octahedra sharing their corners in the xy plane or one layer hexagonal $WO_3$; (b) The hexagonal $WO_3$ structure showing the tunnels along the z axis; the relevant right structures are three membered ring cases [18].

### 1.2.3 Application of Tungsten Oxide [1-7, 19]

$WO_3$ is a versatile wide band-gap semiconductor for many valuable applications. It is considered as a promising material for a multiple of potential applications including semiconductors, gas sensors, cathode materials for secondary batteries, solar energy devices, photocatalysts, erasable optical storage devices and field-emission devices. Generally, monoclinic tungsten oxide structure (m-$WO_3$), is used in gas sensors. In particular, the hexagonal tungsten oxide structure (h-$WO_3$) as tunnel structure is of great interesting due to small ions such as $H^+$, $Li^+$, $Na^+$, $K^+$, etc , which can be inserted in an intercalation host of tunnel h-$WO_3$ to produce tungsten oxide bronzes. The energy was obtained by the reversed reaction. Therefore, it is a

candidate for electrocatalysis for hydrogen evolution reaction of fuel cells, and cathodes for secondary Li-ion batteries.

### 1.3 Hydrothermal / Solvothermal method [20]

The hydrothermal technique is becoming one of the most important tools for advanced materials processing, particularly owing to its advantages in the processing of nanostructural materials for a wide variety of technological applications such as electronics, optoelectronics, catalysis, ceramics, magnetic data storage, biomedical, biophotonics, etc. The hydrothermal technique not only helps in processing monodispersed and highly homogeneous nanoparticles, but also acts as one of the most attractive techniques for processing nano-hybrid and nanocomposite materials. The term 'hydrothermal' is purely of geological origin. It was first used by the British geologist, Sir Roderick Murchison (1792-1871) to describe the action of water at elevated temperature and pressure, in bringing about changes in the earth's crust leading to the formation of various rocks and minerals. It is well known that the largest single crystal formed in nature (beryl crystal of >1000 g) and some of the large quantity of single crystals created by man in one experimental run (quartz crystals of several 1000s of g) are both of hydrothermal origin [20].

Hydrothermal processing can be defined as any heterogeneous reaction in the presence of aqueous solvents or mineralizers under high pressure and temperature conditions to dissolve and recrystallize (recover) materials that are relatively insoluble under ordinary conditions. Definition for the word hydrothermal has undergone

several changes from the original Greek meaning of the words ‘hydros’ meaning water and ‘thermos’ meaning heat. Recently, Byrappa and Yoshimura define hydrothermal as any heterogeneous chemical reaction in the presence of a solvent (whether aqueous or non-aqueous) above the room temperature and at pressure greater than 1 atm in a closed system. However, there is still some confusion with regard to the very usage of the term hydrothermal. For example, chemists prefer to use a term, viz. solvothermal, meaning any chemical reaction in the presence of a non-aqueous solvent or solvent in supercritical or near supercritical conditions. Similarly there are several other terms like glycothermal, alcothermal, ammonothermal, and so on. Further, the chemists working in the supercritical region dealing with the materials synthesis, extraction, degradation, treatment, alteration, phase equilibria study, etc., prefer to use the term supercritical fluid technology. However, if we look into the history of hydrothermal research, the supercritical fluids were used to synthesize a variety of crystals and mineral species in the late 19th century and the early 20th century itself. So, a majority of researchers now firmly believe that supercritical fluid technology is nothing but an extension of the hydrothermal technique. Hence, here the authors use only the term hydrothermal throughout the text to describe all the heterogeneous chemical reactions taking place in a closed system in the presence of a solvent, whether it is aqueous or non-aqueous [20].



The term advanced material is referred to a chemical substance whether organic or inorganic or mixed in composition possessing desired physical and chemical properties. In the current context the term materials processing is used in a very broad sense to cover all sets of technologies and processes for a wide range of

industrial sectors. Obviously, it refers to the preparation of materials with a desired application potential. Among various technologies available today in advanced materials processing, the hydrothermal technique occupies a unique place owing to its advantages over conventional technologies. It covers processes like hydrothermal synthesis, hydrothermal crystal growth leading to the preparation of fine to ultra fine crystals, bulk single crystals, hydrothermal transformation, hydrothermal sintering, hydrothermal decomposition, hydrothermal stabilization of structures, hydrothermal dehydration, hydrothermal extraction, hydrothermal treatment, hydrothermal phase equilibria, hydrothermal electrochemical reactions, hydrothermal recycling, hydrothermal microwave supported reactions, hydrothermal mechanochemical, hydrothermal sonochemical, hydrothermal electrochemical processes, hydrothermal fabrication, hot pressing, hydrothermal metal reduction, hydrothermal leaching, hydrothermal corrosion, and so on. The hydrothermal processing of advanced materials has lots of advantages and can be used to give high product purity and homogeneity, crystal symmetry, metastable compounds with unique properties, narrow particle size distributions, a lower sintering temperature, a wide range of chemical compositions, single-step processes, dense sintered powders, sub-micron to nanoparticles with a narrow size distribution using simple equipment, lower energy requirements, fast reaction times, lowest residence time, as well as for the growth of crystals with polymorphic modifications, the growth of crystals with low to ultra low solubility, and a host of other applications [20].

In the 21st century, hydrothermal technology, on the whole, will not be just limited to the crystal growth, or leaching of metals, but it is going to take a very broad shape covering several interdisciplinary branches of science. Therefore, it has to be

viewed from a different perspective. Further, the growing interest in enhancing the hydrothermal reaction kinetics using microwave, ultrasonic, mechanical, and electrochemical reactions will be distinct. Also, the duration of experiments is being reduced at least by 3-4 orders of magnitude, which will in turn, make the technique more economic. With an ever-increasing demand for composite nanostructures, the hydrothermal technique offers a unique method for coating of various compounds on metals, polymers and ceramics as well as for the fabrication of powders or bulk ceramic bodies. It has now emerged as a frontline technology for the processing of advanced materials for nanotechnology. On the whole, hydrothermal technology in the 21st century has altogether offered a new perspective which is illustrated in Figure 1.4 It links all the important technologies like geotechnology, biotechnology, nanotechnology and advanced materials technology. Thus it is clear that the hydrothermal processing of advanced materials is a highly interdisciplinary subject and the technique is popularly used by physicists, chemists, ceramists, hydrometallurgists, materials scientists, engineers, biologists, geologists, technologists, and so on. Figure 1.5 shows various branches of science either emerging from the hydrothermal technique or closely linked with the hydrothermal technique. One could firmly say that this family tree will keep expanding its branches and roots in the years to come [20].



The hydrothermal processing of materials is a part of solution processing and it can be described as super heated aqueous solution processing. Figure 1.6 shows the PT map of various materials processing techniques. According to this, the hydrothermal processing of advanced materials can be considered as environmentally benign. Besides, for processing nanomaterials, the hydrothermal technique offers

special advantages because of the highly controlled diffusivity in a strong solvent media in a closed system. Nanomaterials require control over their physico-chemical characteristics, if they are to be used as functional materials. As the size is reduced to the nanometer range, the materials exhibit peculiar and interesting mechanical and physical properties: increased mechanical strength, enhanced diffusivity, higher specific heat and electrical resistivity compared to their conventional coarse grained counter-parts due to a quantization effect [20].

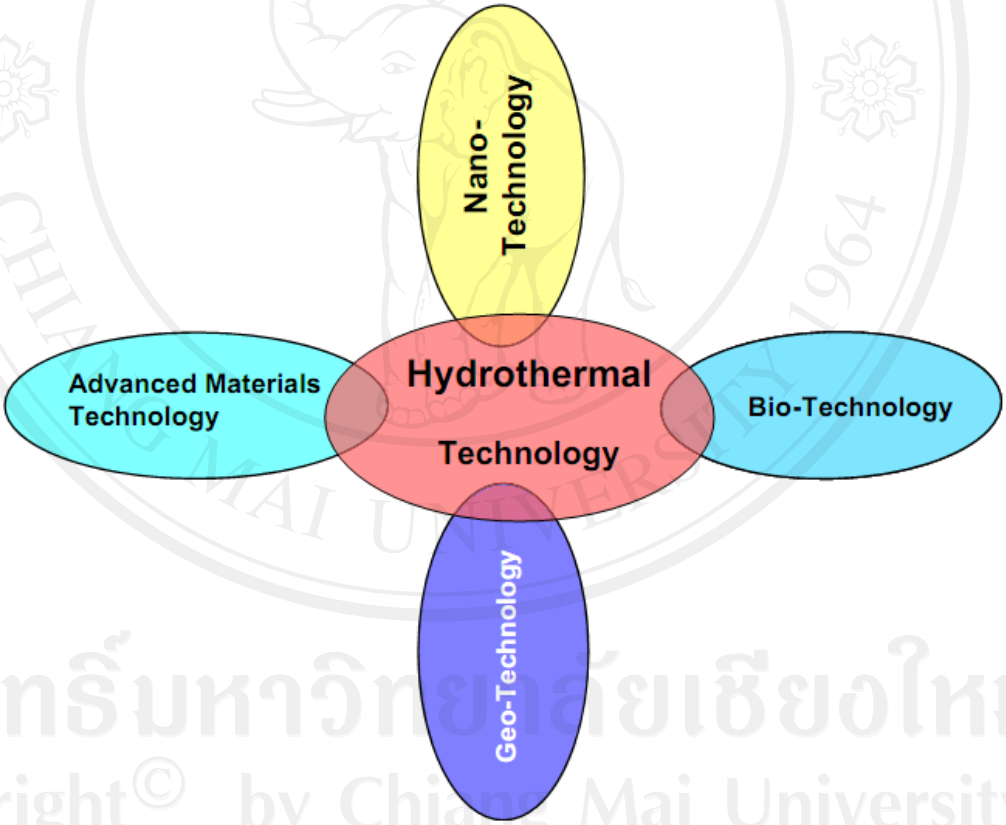


Figure 1.4 Hydrothermal technology in the 21st century [20].

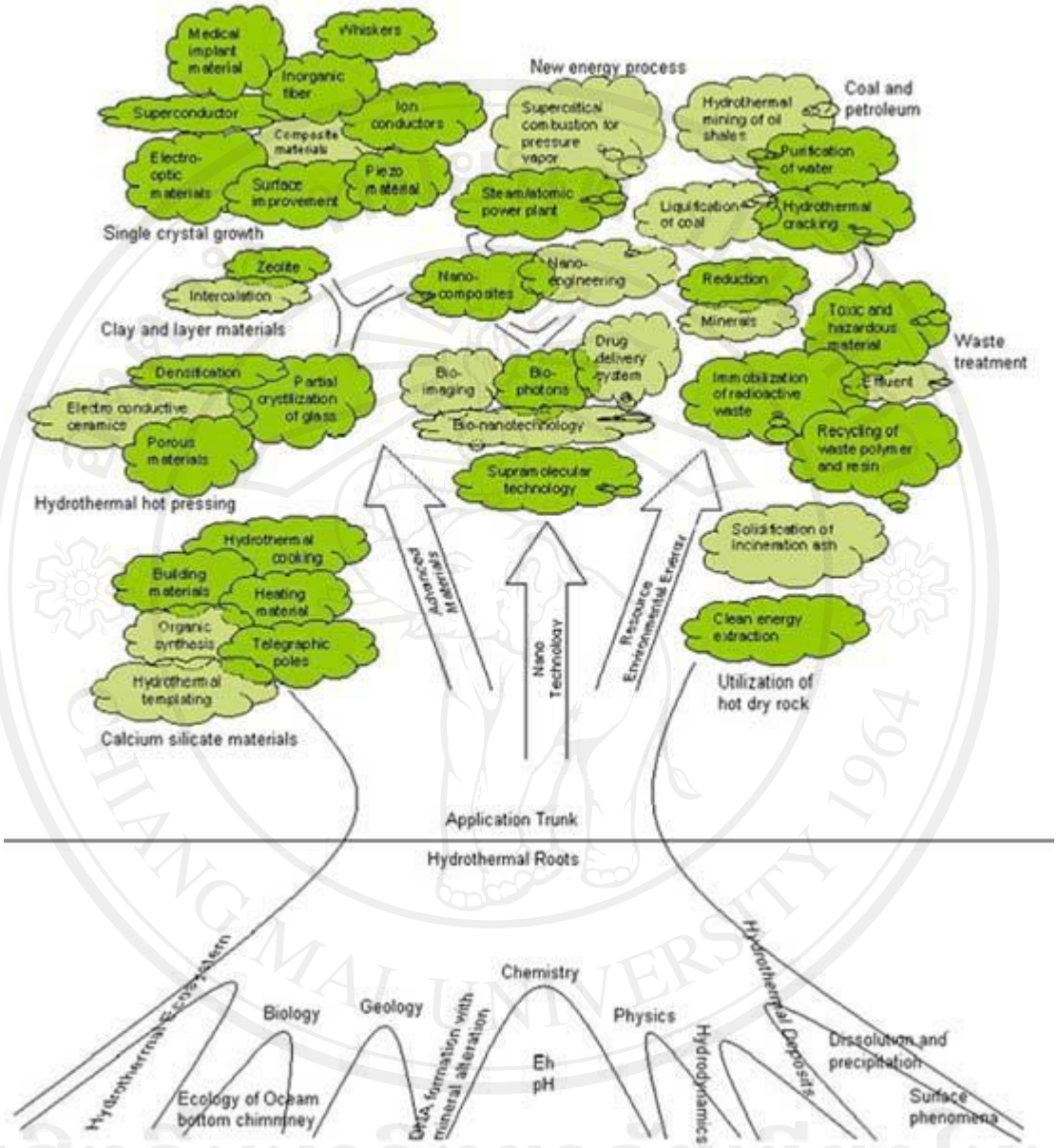


Figure 1.5 Hydrothermal tree showing different branches of science and technology [20].

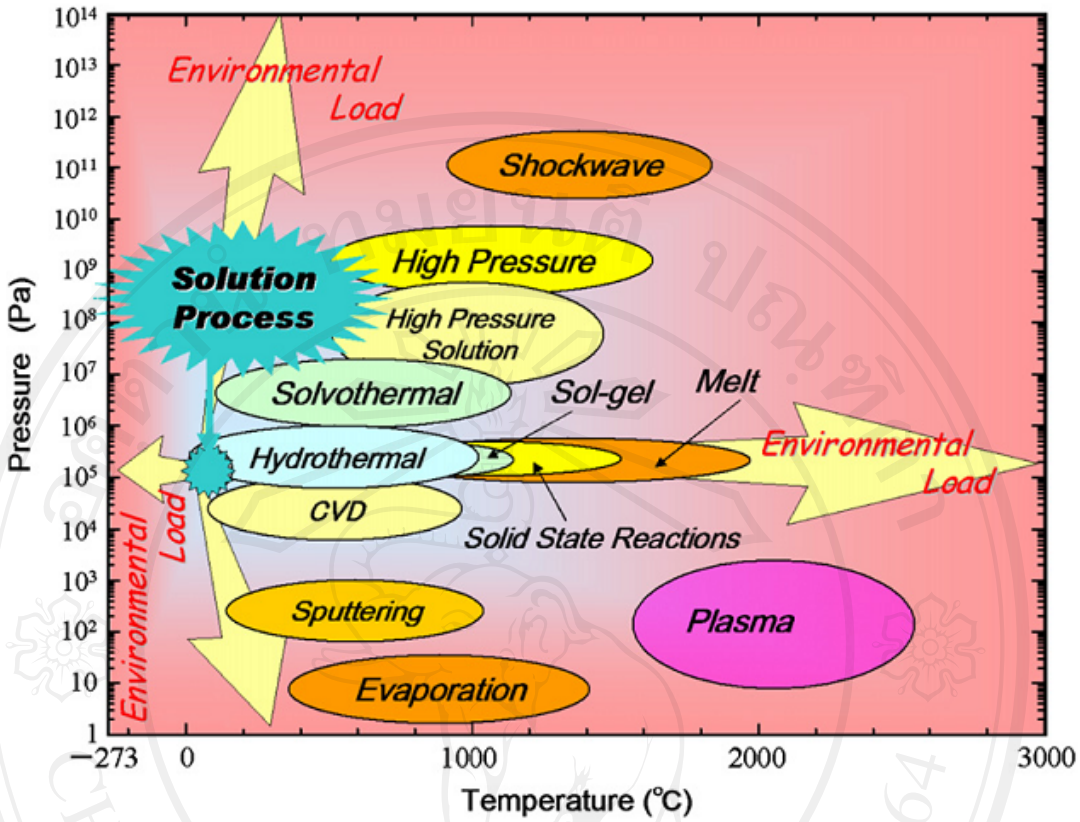


Figure 1.6 Pressure temperature map of materials processing techniques [20].

Hydrothermal technology as mentioned earlier in a strict sense also covers supercritical water or supercritical fluid technology, which is gaining momentum in the last 1½ decades owing to its enormous advantages in the yield and speed of production of nanoparticles and also in the disintegration, transformation, recycling and treatment of various substances including toxic organics, wastes, etc. In case of supercritical water technology, water is used as the solvent in the system, whereas supercritical fluid technology is a general term when solvents like $CO_2$ and several other organic solvents are used, and because these solvents have lower critical temperature and pressure compared to water this greatly helps in processing the

materials at much lower temperature and pressure conditions. Hence, chemists use the term green chemistry for materials processing using supercritical fluid technology. Arai *et al.* (Japan) and Krukonis *et al.* (USA), Poliakoff (UK), Perrut and Cansell (France), Han (China), Yoo and Lee (South Korea), etc., have done extensive studies in the area of supercritical fluid technology [20].

Supercritical water (SCW) and supercritical fluids (SCF) provide an excellent reaction medium for hydrothermal processing of nanoparticles, since they allow varying the reaction rate and equilibrium by shifting the dielectric constant and solvent density with respect to pressure and temperature, thus giving higher reaction rates and smaller particles. The reaction products are to be stable in SCF leading to fine particle formation. The hydrothermal technique is ideal for the processing of very fine powders having high purity, controlled stoichiometry, high quality, narrow particle size distribution, controlled morphology, uniformity, less defects, dense particles, high crystallinity, excellent reproducibility, controlled microstructure, high reactivity with ease of sintering and so on [20].

Further, the technique facilitates issues like energy saving, the use of larger volume equipment, better nucleation control, avoidance of pollution, higher dispersion, higher rates of reaction, better shape control, and lower temperature operations in the presence of the solvent. In nanotechnology, the hydrothermal technique has an edge over other materials processing techniques, since it is an ideal one for the processing of designer particulates. The term designer particulates refers to particles with high purity, high crystallinity, high quality, monodispersed and with controlled physical and chemical characteristics. Today such particles are in great

demand in industries. Figure 1.7 shows the major differences in the products obtained by ball milling or sintering or firing and by the hydrothermal method. In this respect hydrothermal technology has the sign of progress in the last decade in processing a great variety of nanomaterials ranging from microelectronics to micro-ceramics and composites. Here the authors discuss the progress made in the area of hydrothermal technology for the past one decade in the processing of advanced nanomaterials. These materials, when put into proper use, will have a profound impact on our economy and society at least in the early part of 21st century, comparable to that of semiconductor technology, information technology or cellular and molecular biology. It is widely speculated that the nanotechnology will lead to the next industrial revolution. Though it is widely believed that commercial nanotechnology is still in its infancy, the rate of technology enablement is increasing in no small part, as substantial government mandated funds have been directed toward nanotechnology. It is strongly believed that hydrothermal technology has a great prospect especially with respect to nanotechnology research [20].

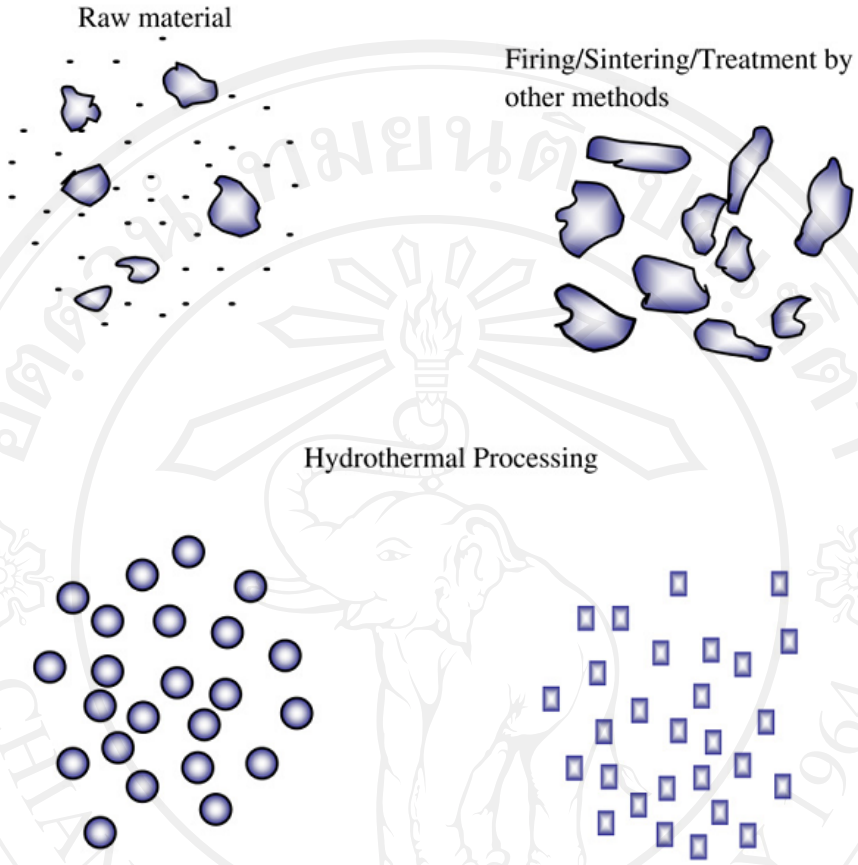


Figure 1.7 Difference in particle processing by hydrothermal and conventional techniques [20].

Figure 1.8 General purpose autoclave popularly used for hydrothermal treatment and synthesis [20].

**1.4 Surfactant** [21]

The term surfactant is a shortened form of "surface active agent". Surfactants are usually organic compounds that are amphiphilic, meaning they contain both hydrophobic tail portion groups usually a long-chain hydrocarbon and hydrophilic polar head groups, which is often ionic (see Figure 1.9). Therefore, they are soluble in both organic solvents and water. Surfactants have the properties to reduce the surface tension of water by adsorbing at the liquid-gas interface. They are able to reduce the interfacial tension between oil and water by adsorbing at the liquid-liquid interface as well [21].

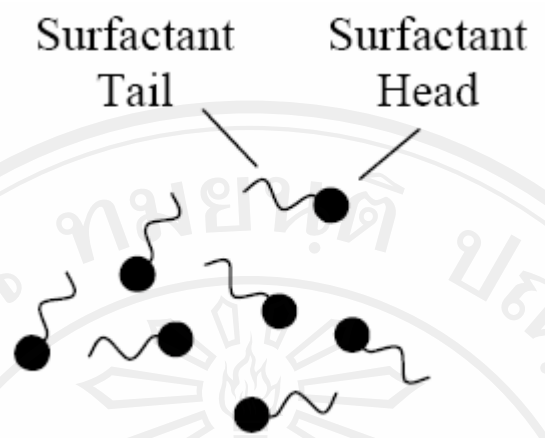


Figure 1.9 Schematic illustration of the micelle monomers. The black circles represent the surfactant heads (hydrophilic moieties) and the black curved lines represent the surfactant tails (hydrophobic moieties) [21].

A surfactant can be classified by the presence of formally charged groups in its head. A nonionic surfactant has no charge groups in its head. The head of an ionic surfactant carries a net charge. If the charge is negative, the surfactant is more specifically called anionic; if the charge is positive, it is called cationic. If a surfactant contains a head with two oppositely charged groups, it is termed zwitterionic. Some commonly encountered surfactants of each type include [21]:

1) Ionic surfactant

1.1) Anionic (based on sulfate, sulfonate or carboxylate anions)

- Sodium dodecyl sulfate (SDS), ammonium lauryl sulfate, and other alkyl sulfate salts
- Sodium laureth sulfate, also known as sodium lauryl ether sulfate (SLES)

- Alkyl benzene sulfonate
- Soaps, or fatty acid salts (see acid salts)

1.2) Cationic (based on quaternary ammonium cations)

- Cetyl trimethylammonium bromide (CTAB) a.k.a. hexadecyl trimethyl ammonium bromide, and other alkyltrimethylammonium salts
- Cetylpyridinium chloride (CPC)
- Polyethoxylated tallow amine (POEA)
- Benzalkonium chloride (BAC)
- Benzethonium chloride (BZT)

1.3) Zwitterionic (amphoteric) surfactant

- Dodecyl betaine
- Dodecyl dimethylamine oxide
- Cocamidopropyl betaine
- Coco ampho glycinate

1.4) Nonionic surfactant

- Alkyl poly(ethylene oxide)
- Alkyl polyglucosides, including: Octyl glucoside, Fatty alcohols, Cetyl alcohol and Oleyl alcohol

Table 1.1 Surfactant classifications [22]

| | Hydrophobic | Hydrophilic |
|---|---|---|
| *Anionic* | | |
| Sodium dodecanoate | $CH_3(CH_2)_{10}$ | $COO^-Na^+$ |
| Sodium dodecyl (lauryl) sulphate | $CH_3(CH_2)_{11}$ | $OSO_3^-Na^+$ |
| Sodium dioctyl sulphosuccinate | $CH_3(CH_2)_7.OOC.CH$ | $SO_3^-Na^+$ |
| | $CH_3(CH_2)_7.OOC.CH_2$ | |
| *Cationic* | | |
| Hexadecyl trimethyl ammonium bromide (Cetrimide) | $CH_3(CH_2)_{15}$ | $N^+(CH_3)_3Br^-$ |
| Dodecyl pyridinium iodide | $CH_3(CH_2)_{11}$ | $N^+H\ I^-$ |
| *Non-ionic* | | |
| Hexaoxyethylene monohexadecyl ether | $CH_3(CH_2)_{15}$ | $(OCH_2CH_2)_6OH$ |
| Polyoxyethylene sorbitan mono-oleate (polysorbate 80) | $C_{17}H_{33}$ | $COOCH_2 \cdot CH_2(CH_2CH_2O)_nOCH_2$ <br> $HO(CH_2CH_2O)_nCH$ <br> $HO(OCH_2CH_2)_n$ <br> $(CH_2CH_2O)_nOH$ <br> $HO(OCH_2CH_2)_n$ <br> $(CH_2CH_2O)_nOH$ <br> $(CH_3CH_2O)_nOH$ |
| Sorbitan mono-oleate | $C_{17}H_{33}$ | $COOCH_2CH$ <br> $OH$ <br> $HO$ <br> $OH$ |
| *Ampholytic* <br> *N*-dodecyl alanine | $CH_3(CH_2)_{11}$ | $NH_2.CH_2.CH_2.COO^-$ |
| Lecithin | $C_{17}H_{35}$ | $COO.CH_2$ |
| | $C_{17}H_{35}$ | $COO.CH$ <br> $CH_2-O-P(=O)(O^-)-O(CH_2)_2N^+(CH_3)_3$ |

Many surfactants can also assemble in the bulk solution into aggregates. Some of these aggregates are known as micelles. The concentration at which surfactants begin to form micelles is known as the critical micelle concentration (CMC). When micelles form in water, their tails form a core that is like an oil droplet. Their (ionic/polar) heads form an outer shell that maintains favorable contact with water. When surfactants assemble in oil, the aggregate is referred to as a reverse micelle of which the heads are in the core and the tails maintain favorable contact

with oil. Micelles are labile entities formed by the noncovalent aggregation of individual surfactant monomers and can be spherical, cylindrical, or planar (discs or bilayers). Micelle shape and size can be controlled by changing the surfactant chemical structure as well as by varying solution conditions, including temperature, overall surfactant concentration, surfactant composition (in the case of mixed surfactant systems), ionic strength, and pH. In particular, depending on the surfactant type and on the solution conditions, spherical micelles can grow one-dimensionally into cylindrical micelles or two dimensionally into bilayers or discoidal micelles [21].

Different concentrations of surfactants can form micelles with different morphologies, which result in the modification of crystal growth. When the concentration of surfactant is larger than that of the CMC, micelles will be formed in the aqueous solutions. At a lower concentration of surfactant, spherical micelles are formed. However, at higher concentration of surfactant, sandwich micelles are formed [23]. Micelle growth is controlled primarily by the surfactant heads, since both one-dimensional and two-dimensional growth require bringing the surfactant heads closer to each other in order to reduce the available area per surfactant molecule at the micelle surface, and hence the curvature of the micelle surface (see Figure 1.10) [24].

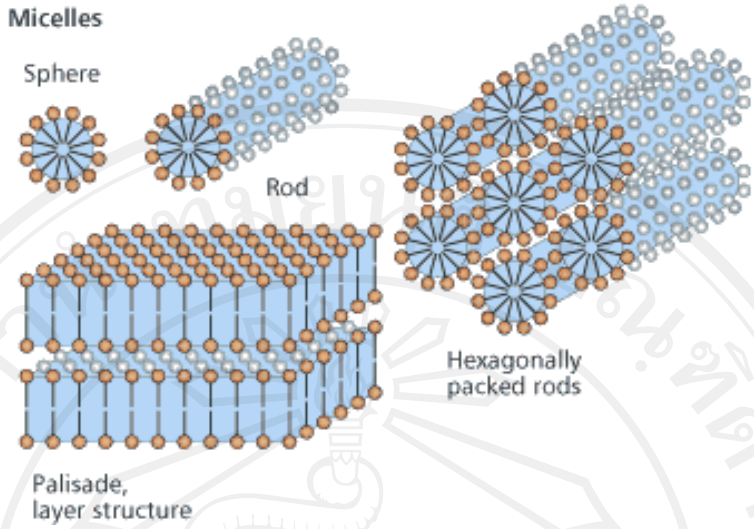


Figure 1.10 Schematic illustration of the commonly observed geometrical shapes of surfactant micelles in aqueous solution. When micelles form in aqueous solution above the CMC, the surfactant monomers aggregate (self-assemble) with the tails inside the micelle shielded from water and the heads at the micelle surface in contact with water [24].

## 1.5 Literature Review

Song *et al.* [8] have hydrothermally fabricated tungsten oxide nanobelts at 180 °C for 12 h by using tungstic acid ($H_2WO_4$) as tungsten source, and sodium sulfide ($Na_2S$) and cetyltrimethylammonium bromide (CTAB) which acted corporately during the nanobelt formation. X-ray diffraction (XRD) patterns indicate that the as-prepared samples are pure orthorhombic $WO_3$ phase. EDS spectra show that the ratio of W/O is about 1:3. The morphology was characterized by scanning electron microscopy (SEM) and transmission electron microscopy (TEM). Based on a

series of comparative experiments under different reaction conditions, the probable formation mechanism of tungsten oxide nanobelts is proposed.

Mo *et al.* [16] have prepared tungsten oxide nanorods at 453 K by the hydrothermal treatment of aqueous tungstic acid solution, which was obtained by passing sodium tungstate solution through a strongly acidic ion-exchange resin. The composition and morphology evolution of the nanorods were investigated by means of scanning electron microscopy, transmission electron microscopy, selected area electron diffraction and X-ray diffraction. The results show that all as-prepared samples mainly consist of hexagonal tungsten oxide and tungsten oxide one-third hydrate. With the extension of treatment time, the sample morphology will undergo an evolution in the sequence of nanorods, bundle-like and irregular shapes.

Song *et al.* [9] have fabricated $WO_3$ nanowires by a hydrothermal method in the presence of $K_2SO_4$. The nanowires exhibit a well crystallized one dimensional structure with 10 nm in diameter and several microns in length. Effect of other alkali salts ($KNO_3$, $NaNO_3$ and $Na_2SO_4$) on the morphologies of $WO_3$ nanocrystals was also investigated. The important role of $K_2SO_4$ salt in the $WO_3$ nanowires synthesis has been demonstrated.

Gu *et al*. [3] have successfully prepared single-crystal nanowires of hexagonal tungsten oxide in a large scale by a simple hydrothermal method without any templates and catalysts. Uniform h-$WO_3$ nanowires with diameter of 25–50 nm and length of up to several micrometers were obtained. It was found that the morphology and crystal formation processes of the final products are strongly dependent on the amount of the sulfate and pH value of the reaction system. The electrochemical

performances of the as-prepared h-$WO_3$ nanowires as anodic materials of Li-ion batteries have also been investigated. It delivers a discharge capacity of 218 mA.h.$g^{-1}$ for the first cycle. In addition, the cycle ability of the nanocrystals is superior to that of bulk materials, which implies the morphology and particle size influencing on the electrochemical performances.

Ha *et al.* [6] have synthesized 1D self-assembled single-crystalline hexagonal tungsten oxide (h-$WO_3$) nanostructures by a hydrothermal method at 180 °C using sodium tungstate, sodium or ammonium ethylenediaminetetraacetate (EDTA) salts, and sodium sulfate. Controlled morphological modification of h-$WO_3$ nanowire bundles was achieved and hierarchical urchin-like structures were produced by simply substituting the sodium ions with ammonium ions in the EDTA salt solution. Self-assembled h-$WO_3$ nanowire bundles and nanorods that formed urchin-like structures were characterized by X-ray diffraction (XRD), scanning electron microscopy (SEM), and transmission electron microscopy (TEM). 1D self-assembled h-$WO_3$ nanowire bundles of ~100 nm diameter and 1–2 μm long were comprised of several individual uniform nanowires of 4–6 nm diameter. These individual nanowires served as building blocks of the bundles. Cyclic voltammetry (CV), and photoluminescence (PL) spectroscopy studies revealed their good electrochemical and luminescence properties. The synthesis of 1D self-assembled h-$WO_3$ nanowire bundles and urchin-like structures was differentiated by means of $Na^+$- and $NH_4^+$-based EDTA salt solutions.

Huirache-Acuña *et al.* [10] have successfully synthesized nanostructures of tungsten oxide ($WO_3$) by using an aged route at low temperature (60 °C), followed by

a hydrothermal method at 200 °C for 48 h under well controlled conditions. The material was studied by X-ray diffraction (XRD), scanning electron microscopy (SEM) and energy dispersive spectroscopy (EDS), transmission electron microscopy (TEM) and high-resolution transmission electron microscopy (HRTEM), Raman spectroscopy and X-ray photoelectron spectroscopy (XPS). Specific surface areas were measured by using the BET method. The lengths of the $WO_3$ nanostructures obtained are between 30 and 200 nm and their diameters are from 20 to 70 nm. The growth direction of the tungsten oxide nanostructures was determined along the [010] axis with an interplanar distance of 0.38 nm.

Rajagopal *et al.* [25] have synthesized tungsten oxide ($WO_3$) nanostructures by hydrothermal method using sodium tungstate ($Na_2WO_4.2H_2O$) alone as starting material, and sodium tungstate in presence of ferrous ammonium sulfate [$(NH_4)_2Fe(SO_4)_2.6H_2O$] or cobalt chloride ($CoCl_2.6H_2O$) as structure-directing agents. Orthorhombic $WO_3$ having a rectangular slab-like morphology was obtained when $Na_2WO_4.2H_2O$ was used alone. When ferrous ammonium sulfate and cobalt chloride were added to sodium tungstate, hexagonal $WO_3$ nanowire clusters and hexagonal $WO_3$ nanorods were obtained, respectively. The crystal structure and orientation of the synthesized products were studied by X-ray diffraction (XRD), micro-Raman spectroscopy, and high-resolution transmission electron microscopy (HRTEM), and their chemical composition was analyzed by X-ray photoelectron spectroscopy (XPS). The optical properties of the synthesized products were verified by UV–Vis and photoluminescence studies. A photodegradation study on Procion Red MX

Phuruangrat *et al.* [2] have prepared hexagonal $WO_3$ (h-$WO_3$) nanowires with high aspect ratio and crystallinity by a microwave-assisted hydrothermal method. By using X-ray diffraction, scanning electron microscopy, transmission electron microscopy and high resolution transmission electron microscopy, phase and morphology of the products were identified, which were controlled by reaction temperature, holding time and added salts. Uniform h-$WO_3$ nanowires with a diameter of 5-10 nm and lengths of up to several micrometers were synthesized by a microwave-assisted hydrothermal process in a solution containing $(NH_4)_2SO_4$ as a capping reagent, and $Na_2WO_4$ as a starting material at 150 $^oC$ for 3 h. The aspect ratio and specific surface area of h-$WO_3$ nanowires are 625 and 139 $m^2.g^{-1}$, respectively, which represent one of the highest values among the reported $WO_3$ based materials. The electrocatalytic activity for hydrogen evolution reaction of h-$WO_3$ nanowires has also been investigated by a cyclic voltammetry and linear sweep voltammetry. They were demonstrated that h-$WO_3$ nanowires are promising electrocatalysts for hydrogen evolution reaction (HER) from water.

Salmaoui *et al.* [11] have synthesized hexagonal tungsten oxide nanorods by hydrothermal route using $Na_2WO_4.2H_2O$ as tungsten source, $C_6H_5NH_2$ and sodium sulfate as structure-directing templates. X-ray diffraction (XRD), scanning electron microscopy (SEM), transmission electron microscopy (TEM), high-resolution transmission electron microscopy (HRTEM), Fourier transform infrared spectroscopy (FTIR) and Raman spectroscopy have been used to characterize the structure, morphology and vibration of the nanorods. The h-$WO_3$ nanorods are up to 5 μm in length, and 50–70 nm in diameter.

Yan *et al.* [26] have successfully synthesized tungsten oxide hydrate nanowire netted-spheres in the glycol solution using a facile solvothermal approach. The nanowires with uniform diameter of 4–6 nm are actually a kind of tungsten oxide hydrate/surfactant hybrid materials. The influence of surfactant, solvent, time and temperature on tailoring morphology was investigated in detail. The possible formation process of $WO_3$ hydrate nanowire netted-sphere was proposed. Sensing properties of such $WO_3$ hydrate sensor show that the desirable sensing characteristics towards 100 ppm ammonia gas at 320 $^oC$ were obtained, such as rapid response (18.3 s), high sensitivity, good reproducibility and stability.

Bi *et al.* [27] have successfully prepared tungsten oxides with different morphologies including platelet-like sheets, nanobelts, and nanoparticles by changing the ions in the synthetic solution. Transmission electron microscopy, X-ray diffraction, Fourier-transform infrared analysis and $N_2$ adsorption were employed to reveal the morphological evolution, and results show that the morphological evolution can be attributed to the alteration of coordination environment of tungstenic cations contained in the synthetic solution. Furthermore, these products have been applied into hydrodesulfurization measurement to investigate the relationship between the morphologies of tungsten oxides and their catalytic properties. It is concluded that the catalysts originating from nanobelt-like tungsten oxides have highest catalytic activity and excellent selectivity due to their scrolled character and strong metallic edges.

Li *et al.* [28] have prepared tungsten oxide nanorods by a simple microwave hydrothermal (MH) method via $Na_2SO_4$ as structure-directing agent at 180 $^oC$ for 20 min. The structure and morphology of the products are characterized by X-ray powder

diffraction (XRD) and transmission electron microscopy (TEM). The obtained nanorods are about 20–50 nm in diameter and several micrometers in length. The ethanol sensing property of as-prepared tungsten oxide nanorods is studied at ethanol concentration of 10–1000 ppm and working temperature of 370–500 $^{o}$C. It was found that the sensitivity depended on the working temperatures and also ethanol concentration. The results show that the tungsten oxide nanorods can be used to fabricate high performance ethanol sensors.

**1.6 Research Objectives**

1.6.1 To synthesize and characterize $WO_3$ nanostructure by hydrothermal method.

1.6.2 To study the influence of acidity, reaction temperature, time on the phase, morphologies and optical properties of $WO_3$ nanostructure.